# *In vivo* optical biopsy of hamster oral cavity with epi-third-harmonic-generation microscopy

**Shih-Peng Tai**

*Department of Electrical Engineering and Graduate Institute of Electro-Optical Engineering, National Taiwan University, Taipei 10617, Taiwan*

**Wen-Jeng Lee**

*Department of Electrical Engineering National Taiwan University and Department of Medical Imaging, National Taiwan University Hospital, Taipei 10617, Taiwan*

**Dar-Bin Shieh and Ping-Ching Wu**

*Institute of Oral Medicine and Institute of Basic Medical Sciences, Center for Micro/Nano Sciences and Technology,, National Cheng-Kung University, Tainan, Taiwan*

**Hsin-Yi Huang**

*Department of Pathology, National Taiwan University Hospital, Taipei 10617, Taiwan*

**Che-Hang Yu and Chi-Kuang Sun***

*Department of Electrical Engineering and Graduate Institute of Electro-Optical Engineering, National Taiwan University, Taipei 10617, Taiwan*
*sun@cc.ee.ntu.edu.tw*

**Abstract**: The first *in vivo* optical virtual biopsy based on epi-third-harmonic-generation (THG) microscopy is successfully demonstrated using Syrian hamster oral mucosa as a model system. Without complex physical biopsy procedures, epi-THG microscopy can provide high spatial resolution dynamic images of oral mucosa and sub-mucosa in all three dimensions. The demonstrated intra-vital epi-THG microscopy provide high resolution observation of blood flow in the capillary and could be a promising tool to image angiogenesis, which is an important feature for many human diseases including malignancies. The system setup of epi-THG microscopy can be easily integrated with other nonlinear optical microscopy such as second-harmonic generation and multi-photon fluorescence microscopy by using the same laser system to provide better integrated molecular and structural information for future clinical diagnosis. By adding 6% acetic acid solution on the mucosa, THG contrast on the borders of nuclei was found to be greatly enhanced due to the alterations of their linear and nonlinear THG susceptibilities. With a virtual-transition-based technology without using fluorescence, the optical epi-THG biopsy we demonstrated shows promise for future noninvasive *in vivo* diseases examinations.



**OCIS codes**: (180.6900) Three-dimensional microscopy; (180.5810) Scanning microscopy; (190.4160) Multiharmonic generation

## References and links

1. D. Yelin and Y. Silberberg, "Laser scanning third-harmonic-generation microscopy in biology," Opt. Express **5**, 169-175 (1999.

#70983 - $15.00 USD Received 15 May 2006; revised 6 June 2006; accepted 8 June 2006

2. S.-W. Chu, I.-S. Chen, T.-M. Liu, C.-K. Sun, S.-P. Lee, B.-L. Lin, P.-C. Cheng, M.-X. Kuo, D.-J. Lin, and H.-L. Liu, "Nonlinear bio-photonic crystal effects revealed with multi-modal nonlinear microscopy," J. Microsc. **208**, Part 3, 190-200 (2002).
3. C.-K. Sun, C.-C. Chen, S.-W. Chu, T.-H. Tsai, Y.-C. Chen and B.-L. Lin, "Multi-harmonic-generation biopsy of skin," Opt. Lett. **28**, 2488-2490 (2003).
4. S.-P. Tai, T.-H. Tsai, W.-J. Lee, D.-B. Shieh, Y.-H. Liao, H.-Y. Huang, K. Y.-J. Zhang, H.-L. Liu, and C.-K. Sun, "Optical biopsy of fixed human skin with backward-collected optical harmonics signals," Opt. Express **13**, 8231-8242 (2005).
5. T.-H Tsai, S.-P. Tai, W.-J. Lee, H.-Y. Huang, Y.-H. Liao and C.-K. Sun, "Optical signal degradation study in fixed human skin using confocal microscopy and higher-harmonic optical microscopy," Opt. Express **14**, 749-758 (2006).
6. V. Barzda, C. Greenhalgh, J. Aus der Au, S. Elmore, J. H. van Beek, and J. Squier, "Visualization of mitochondria in cardiomyocytes by simultaneous harmonic generation andfluorescence microscopy," Opt. Express **13**, 8263-8276 (2005).
7. D. Debarre, W. Supatto, A.-M. Pena, A. Fabre, T. Tordjmann, L. Combettes, M.-C. Schanne-Klein, and E. Beaurepaire, "Imaging lipid bodies in cells and tissues using third-harmonic generation microscopy," Nat. Methods **3**, 47-53 (2006).
8. C.-K. Sun, S.-W. Chu, S.-Y. Chen, T.-H. Tsai, T.-M. Liu, C.-Y. Lin, and H.-J. Tsai, "Higher harmonic generation microscopy for developmental biology," J. Struct. Biol. **147**, 19-30 (2004).
9. L. Canioni, S. Rivet, L. Sarger, R. Barille, P. Vacher, and P. Voisin, "Imaging of Ca2+ intracellular dynamics with a third-harmonic generation microscope," Opt. Lett. **26**, 515-517 (2001).).
10. T.-M. Liu, S.-W Chiu, C.-K Sun, B.-L. Lin, P. C. Cheng, and I. Johnson, "Multi-photon scanning microscopy using a femtosecond Cr:forsterite laser," Scanning **23**, 249-254 (2001).
11. G. Peleg, A. Lewis, M. Linial, and L. M. Loew "Nonlinear optical measurement of membrane potential around single molecules at selected celluar sites," Proc. Natl. Acad. Sci. **96**, 6700-6704 (1999).
12. J. A. Squier, M. Muller, G. J. Brakenhoff, and K. R. Wilson, "Third harmonic generation microscopy," Opt. Express **3**, 315-324 (1998).
13. I-H. Chen, S.-W. Chu, C.-K. Sun, P.-C. Cheng, and B.-L. Lin, "Wavelength dependent cell damages in biological multi-photon confocal microscopy: A micro-spectroscopic comparison between femtosecond Ti:sapphire and Cr:forsterite laser sources," Opt. Quantum. Electron. **34**, 1251-1266 (2002).
14. P. J. Campagnola, A. C. Millard, M. Terasaki, P. E. Hoppe, C. J. Malone, and W. A. Mohler, "Three-dimensional high-resolution second-harmonic generation imaging of endogenous structural proteins in biological tissues," Biophys. J. **81**, 493-508 (2002).
15. K. H. Kim, C. Buehler, and P. T. C. So, "High speed, two-photon scanning microscope," Appl. Opt. **38**, 6004-6009 (1999).
16. J. X. Cheng, A. Volkmer, L. D. Book, and X. S. Xie, "An epi-detected coherent anti-stokes Raman scattering (E-CARS) microscope with high spectral resolution and high sensitivity," J. Phys. Chem. B **105**, 1277-1280 (2001).
17. A. Volkmer, J. X. Cheng, and X. S. Xie, "Vibrational imaging with high sensitivity via epidetected coherent anti-Stokes Raman scattering microscopy," Phys. Rev. Lett. **87**, 023901 (2001).
18. J. X. Cheng, A. Volkmer, and X. S. Xie, "Theoretical and experimental characterization of coherent anti-Stokes Raman scattering microscopy," J. Opt. Soc. Am. B **19**, 1363-1375 (2002).
19. A. Volkmer, "Vibrational imaging and microspectroscopies based on coherent anti-Stoke Raman scattering microscopy," J. Phys. D: Appl. Phys. **38**, R59-R81 (2005).
20. J. X. Cheng, and X. S. Xie, "Green's function formulation for third-harmonic generation microscopy," J. Opt. Soc. Am. B **19**, 1604-1610 (2002).
21. S.-Y. Chen, S.-P. Tai, T.–H. Tsai and C.–K. Sun, "Direct backward-emitted third-harmonic generation and its application to clinical microscopy", in Technical Digest of Conference on Laser and Electro-optics/Quantum Electronics and Laser Science Conference (CLEO/QELS 2005), Baltimore, MD, USA, paper QMI3 (2005).
22. D. W. Fawcett, *An Atlas of Fine Structure, The cell: Its organelles and inclusions*, (Saunders, Philadelphia 1996).
23. L. T. Perelman, and V. Backman, "Light scattering spectroscopy of epithelial tissue: Principles and applications," *Handbook of Optical Biomedical Diagnostics*, (SPIE, Bellingham, WA 2002) Chap. 12, 675-724.
24. L. Burke, D. Antonioli, B. Durcatman, *Colposcopy Text and Atlas*, (Appleton and Lange., 1991).
25. T. Collier, P. Shen, B. de Pradier, K. -B. Sung, R. Richards-Kortum, M. Follen, and A. Malpica, "Near real time confocal microscopy of amelanotic tissue: Dynamics of aceto-whitening enable nuclear segmentation," Opt. Express **6**, 40-48 (2000).
26. R. A. Drezek, T. Collier, C. K. Brookner, A. Malpica, R. Lotan, R. R. Richards-Kortum, and M. Follen, "Laser scanning confocal microscopy of cervical tissue before and after application of acetic acid," Am. J. Obstet. Gynecol. **182**, 1135-1139 (2000).
27. M. Rajadhyaksha, G. Menaker, T. Flotte, P. J. Dwyer, and S. Gonzalez, "Confocal examinazation of nonmelanoma cancers in thick skin excisions to potentially guide Mohs micrographic surgery without frozen histopathology," J. Invest. Dermatol. **117,** 1137-1143 (2001).

#70983 - $15.00 USD Received 15 May 2006; revised 6 June 2006; accepted 8 June 2006

28. A. A. Lacy, T. Collier, J. E. Price, S. Dharmawardhane and R. R. Richards-Kortum, "Near real-time in vivo confocal imaging of mouse mammary tumors," Front. Biosci. **7**, F1-F7 (2002).
29. A. F. Zuluaga, R. Drzek, T. Collier, R. Lotan, and M. Follen, "Contrast agents for confocal microscopy: how simple chemicals affect confocal images of normal and cancer cells in suspension," J. of Biomed. Opt. **7**, 398-403 (2002).
30. A. N. Yaroslavsky, J. Barbosa, V. Neel, C. DiMarzio, and R. R. Anderson, "Combining multispectral polarized light imaging and confocal microscopy for localization of nonmelanoma skin cancer," J. of Biomed. Opt. **10**, 014011 (2005).
31. K. Carlson, I. Pavlova, M. Descour. M. Follen, and R. R.-Kortum, "Confocal microscopy: Imaging cervical precancerous lesions ," Gynecol. Oncol. **99**, S84-S88 (2005).
32. C.-C. ChangChien, H. Lin, S. W. Leung, C.-Y. Hsu, and C.-L. Cho, "Effect of acetic acid on telomerse acitivity in cervical intraepithelial neoplasia," Gynecol. Oncol. **71**, 99-103 (1998).
33. B. W. Pogue, H. B. Kaufman, A. Zelnechuk, W. Harper, G. C. Burke, E. E. Burke, and D. M. Harper, "Analysis of acetic acid-induced whitening of high-grade squamous intraepithelial lesions," J. of Biomed. Opt. **6**, 397-403 (2001).
34. R. Lambert, J. F. Rey, and R. Sankaranarayanan, "Magnification and chromoscopy with the acetic cid test," Endoscopy **35**, 437-445, (2003).
35. M. Rajadhyaksha, S. Gonzalez, J. M. Zavislan, "Detectability of contrast agents for confocal reflectance imaging of skin and microcirculation," J. of Biomed. Opt. **9**, 323-331 (2002).
36. A. B. MacLean, "Acetowhite epithelium," Gynecol. Oncol. **95**, 691-694 (2004).
37. J. F. Rey, H. Inoue, and M. Guelrud, "Magnification endoscopy with acetic acid for Barrett's esophagus," Endoscopy **37**, 583-586, (2005).
38. W.-J. Lee, C.-H. Yu, S-P. Tai, H.-Y. Huang, and C.-K. Sun, "Functional third-harmonic generation microscopy of cell nuclei by using acetic acid as a contrast agent," in preparation.

## 1. Introduction

In clinical oral diseases diagnosis, physical biopsy is traditionally recognized as the final standard tool. However, physical biopsy requires the removal, fixation, and staining of tissues, cells, or fluids from the lesions of patients. Such histological procedures are not only time-consuming but also invasive and painful. In addition, traditional physical biopsy procedures per se may potentially put patients in the risk of spreading tumor cells. Moreover, unless tedious serial sectionings are performed, there is no guarantee for a missing diagnosis due to a local invasion not present in the given histological sectioning examined by the pathologists. Therefore, a non-invasive *in vivo* optical virtual biopsy, which can provide highly penetrative three-dimensional (3D) images with a sub-micron spatial resolution to assist the real physical biopsy, is highly desired.

Recently, third-harmonic-generation (THG) has been emerged as an important imaging modality in biological researches with the advantages including no energy release due to the characteristic of virtual-state-transition and intrinsic optical sectioning capability due to the nature of third-order nonlinearity. THG imaging has been applied to observe various structures in bio-tissues [1-7] and embryos [8], and to visualize intracellular $Ca^{2+}$ dynamics [9]. Although the third order nonlinearity exists theoretically in all materials, the Gouy phase shift effect substantially limits THG to be observed in the vicinity of interfaces where the first or the third order susceptibilities discontinue. Therefore, THG is an ideal optical biopsy tool to visualize the morphological structures in the bio-tissues because of its interface-sensitive nature.

However, most of previous studies collected THG signals in a forward transmission geometry based on the consideration of momentum conservation [1-3, 5-9]. Unfortunately, for clinical optical biopsy applications, the reflection (or backward scattering) type geometry is preferred for the signal collection due to the optically thick human bodies. Recently, we have demonstrated the optical biopsy of fixed human skin by collecting backward propagating higher harmonics including second harmonic generation (SHG) and THG [4]. From our previous study, we confirmed that epi-SHG and epi-THG microscopies can resolve detailed histological structures from epidermis to dermis with a penetration depth over 350μm [4]. However, our previous work was demonstrated in fixed human specimens so that some tissues

#70983 - $15.00 USD Received 15 May 2006; revised 6 June 2006; accepted 8 June 2006

were still required to be removed from the living bodies and subject to fixation in formalin. This procedure is invasive and the results of the *ex vivo* study may be different from those of *in vivo* physiological conditions because the fixation process may change the optical linear and nonlinear properties and sizes and microstructures of the specimens.

In this paper, the first *in vivo* optical biopsy based on epi-THG microscopy is demonstrated by using live Syrian hamsters as an animal model before human subjects. We confirm the fact that abundant epi-THG signals can be collected from mucosa and sub-mucosa in the hamster oral cavity. Just like forward propagating THG, epi-THG can provide morphological images in both mucosa and sub-mucosa layers with a high spatial resolution, thus providing detailed histological information including the sizes, shapes, and distributions of basal cells. Besides, the movement of red blood cells in the capillary can also be clearly resolved by dynamic epi-THG microscopy. In order to study the origin of the collected epi-THG signals, acetic acid was added into the mucosa to enhance backward scatterings. Our study indicates that the contribution from the direct backward THG emissions should not be neglected, while enhanced epi-THG of nuclear borders can be clearly observed. With a virtual-transition-based technology without using fluorescence, the optical epi-THG biopsy we demonstrated shows promises for noninvasive *in vivo* diseases examinations. Combining with the acetic acid that serves as the THG contrast agent for nuclei, the functional epi-THG microscopy we developed is especially ideal for diagnosing those diseases associated with the nuclear morphology alterations.

## 2. Material and methods

In this study, Syrian hamster is used as our animal model. The experimental protocols were approved by the National Taiwan University Institutional Animal Care and Use Committee (NTU-IACUC). Figure 1(a) shows the schematic setup of our epi-THG microscope. The study of the epi-THG biopsy of the hamster oral cavity was performed using a home-built femtosecond Cr:forsterite laser centered at 1230 nm with a 100 fs pulsewidth and a 110 MHz repetition rate [10]. The spectral full width half maximum of the laser output was about 20nm. The infrared laser beam was first shaped by a telescope and then directed into a modified beam scanning system (Olympus Fluoview300) and an upright microscope (Olympus BX-51). An IR water-immersion objective (Olympus LUMplanFL/IR 60X/NA 0.9/Working distance 2mm) was used to focus the laser beam into the hamster oral cavity. The maximum scanning rate of Fluoview300 is 1000 line/s corresponding to ~two frames per second for a 512×512 resolution. After anaesthetization, the hamster rested in our harmonic optical biopsy (HOB) system [as shown in Fig. 1(b)] with a monitoring system [(as shown in Fig. 1(c)] to maintain the vital signs and the body temperature of the test animal. The epi-THG signals were collected using the same objective. To provide more bio-information in the oral cavity, we also collected epi-SHG signals in this study. We used a chromatic beam splitter, DM1 (Chroma technology 865dcxru), to direct the epi-SHG and epi-THG signals into a home-built photon detection system. In this photon detection system, the SHG and THG signals were divided by another chromatic beam splitter, DM2, and detected by two separate PMTs with 410nm (THG) and 615nm (SHG) narrow band interference filters in front of them. To filter out the fundamental laser wavelength, a color filter (CF) was inserted in the system as shown in Fig. 1(a). The lateral resolution of the epi-THG microscopy in the live hamster oral cavity was analyzed following the method described in a previous work [5]. The measured lateral resolutions, as shown in Fig. 2, were 450-600nm in mucosa and 650-850nm in sub-mucosa, which are similar to our previous results in the fixed human skin specimens [5].

The average laser power illuminated on the test animal was 150 mW, corresponding to a 1.3nJ pulse energy. In our previous studies of *in vivo* vertebrate embryos based on a

#70983 - $15.00 USD Received 15 May 2006; revised 6 June 2006; accepted 8 June 2006

femtosecond Cr:forsterite laser [8], complex developmental processes throughout the 1.5-mm-thick zebrafish embryos from initial cell proliferation, gastrulation, to the tissue formation could all be continuously visualized *in vivo*. No optical damage was found even after a long-term (12-h) continuous observation with 100-mW average incident power onto one embryo, corresponding to a total energy exposure over 1000 J, indicating the least-invasive nature of the higher harmonic generation processes. To evaluate the mammalian cell viability under high average-power femtosecond Cr:forsterite laser illumination in this study, after 3-hours continuous observation under the epi-THG microscope in the same area, the observed hamster buccal tissues were excised immediately and fixed with formalin. Tissues dehydrated and embedded in paraffin were prepared into 5 μm sections and stained with hematoxylin and eosin stain. Histological examinations were then performed under light microscopy by an experienced pathologist. This procedure was repeated for 3 hamsters. The buccal squamous epithelium and sub-epithelial stroma were found to be normal under light microscopy. No evidence of coagulation necrosis could be found.

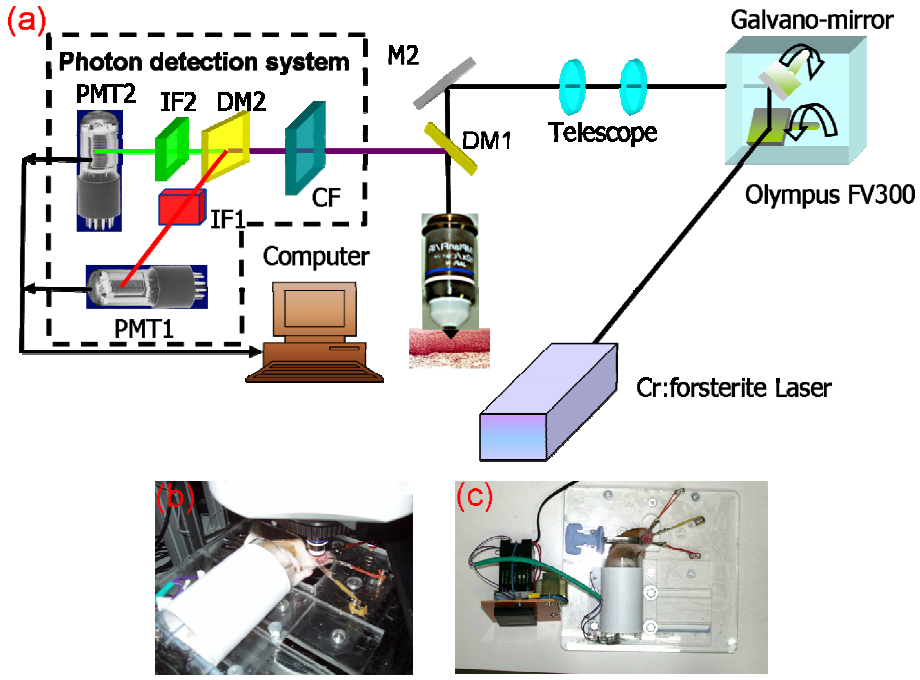


Fig. 1 System setup of harmonics optical biopsy.

#70983 - $15.00 USD
Received 15 May 2006; revised 6 June 2006; accepted 8 June 2006

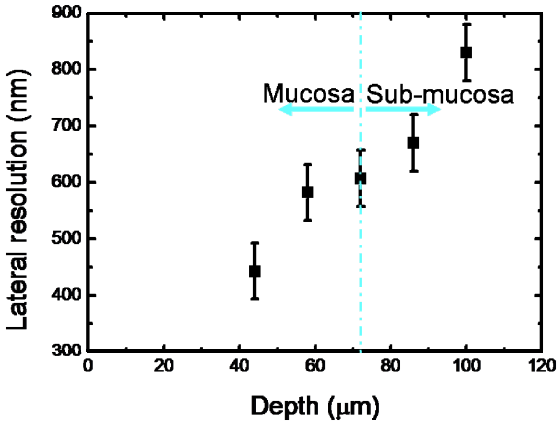


Fig. 2 Measured lateral resolution of *in vivo* epi-THG microscopy vs. depth in hamster oral cavity.

## 3. Results and discussion

### *3.1 Optical virtual biopsy of hamster oral cavity using epi-THG microscopy*

To demonstrate the feasibility for future clinical diagnosis on oral diseases, Fig. 3 shows examples of the horizontally sectioned epi-SHG (green) and epi-THG (red) images taken from the hamster buccal pouch oral mucosa from surface deep into the sub-mucosa layer. From Fig. 3, the general histological structures in both mucosa and sub-mucosa layers can be identified through the THG modality due to its sensitivity to local optical inhomogeneities [1,11,12]. For example, the morphology of stratum corneum (Fig. 3(a), SB), stratum granulosa (Fig. 3(a), SG), stratum basale layer (Fig. 3(b), SB), and red blood cells (Fig. 3(b), RBC) in the capillary can all be easily picked up through the epi-THG microscopy. SHG, on the other hand, mainly reflects the distribution of connective tissues in the sub-mucosa [2, 13, and 14] layer [represented in green color in a. 3(b)] such as lamina propria due to strong SHG generation in collagen fibers. It can be found that the epi-SHG signals are concentrated in the sub-mucosa and can provide information of the structure and distribution of collagen fibrils that may assist clinical diagnosis of connective tissue diseases.

Figures 3 (c) and 3(d) show more detailed microstructures of stratum granulosa and stratum basale provided by the epi-THG microscopy. Clear cell-cell junctions [indicated by yellow arrows in Fig. 3 (d)] between basal cells can be observed. Figure 4 is an example movie showing the blood flow in the capillary imaged by the epi-THG microscopy. The movement of RBCs in the capillary can be clearly resolved. Therefore, epi-THG microscopy can not only provide structure contours and histological information in both mucosa and sub-mucosa but also can monitor the capillary network and the blood flows. This observation indicates that epi-THG microscopy could be an ideal tool to observe angiogenesis, which is not only one of the early signs of caners but also many other important human diseases.

#70983 - $15.00 USD Received 15 May 2006; revised 6 June 2006; accepted 8 June 2006

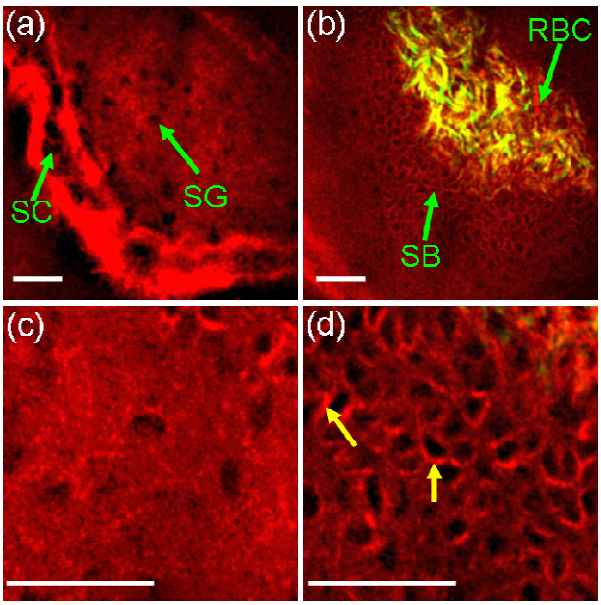


Fig. 3 *In vivo* horizontally sectioned epi-SHG (green) and epi-THG (red) images of hamster mucosa and sub-mucosa taken at different depths. From (a) and (b), we can identify the morphology of stratum corneum (SC), stratum granulosa (SG), stratum basale (SB), and red blood cells (RBC) in the oral cavity by using epi-THG microscopy. Besides, epi-SHG microscopy can provide the distribution and density information of collagen fibrils in the sub-mucosa. At higher magnification, (c) and (d) show more detailed morphologies of stratum granulosa and stratum basale. Clear cell-cell junctions (indicated by yellow arrows) can be picked up by epi-THG microscopy. Scale bar: 40μm.

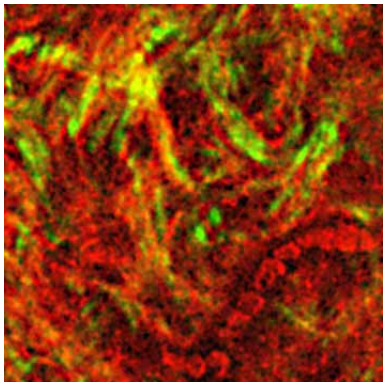

Fig. 4 (1.67 MB) An example movie of the *in vivo* horizontally sectioned epi-THG microscopy showing the blood flow in the capillary in the sub-mucosa layer of the hamster oral cavity. Image size: 80μm×80μm

Figure 5 is an example movie of a sequential set of horizontally sectioned images taken by epi-THG and epi-SHG microscopes. The movie is composed of 30 horizontal sections and the depth difference between two adjacent images is 2.8-μm. Different profiles between two adjacent images can be found. Therefore, this optical biopsy technique enables direct acquisition of high resolution 3-D structural images of the oral cavity and provides an ideal

#70983 - $15.00 USD
Received 15 May 2006; revised 6 June 2006; accepted 8 June 2006

new platform for clinical optical virtual biopsy in the future without using fluorescence and confocal pinhole. The current scanning rate of the system is limited by the speed of the adopted Fluoview300 galvo-mirrors, and real-time epi-THG microscopy can be achieved by using high speed scanners such as polygon mirror scanner [15] to meet the requirements of clinical diagnosis in the future.

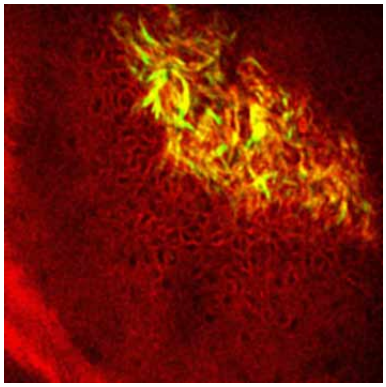

Fig. 5 (1.85 MB) This movie shows a stack of depth-resolved *in vivo* horizontal sections in the hamster oral cavity. Using epi-SHG and epi-THG microscopy, a series of horizontal sections from mucosa to sub-mucosa is demonstrated. This movie is composed of 30 horizontal images. The optical depth difference between adjacent images is 2.8 μm. Image size: 240μm×240μm

### *3.2 Acetic acid as contrast agent of epi-THG microscopy*

With abundant epi-THG signals observed in the oral mucosa and sub-mucosa layers, it is thus highly desirable to investigate the origin of the collected *in vivo* epi-THG signals. The observed epi-THG signals could originate from two mechanisms: direct backward THG emission and the backscattering of forward THG emission. In principle, forward THG should be much stronger than the direct backward THG, thus indicating the un-negligible contribution from the backscattering of forward THG emission. However, the collection of the backscattered THG signals depends on the collection geometry, the scattering length, and the scattering coefficient of the layers underneath. With a high NA objective and a long scattering length, the collection efficiency could be extremely poor. Previous studies in coherent anti-Stoke Raman scattering microscopy, which is another coherent third-order nonlinear microscopy, showed that the direct backward-propagating CARS signals can be generated in a very thin (sub-μm) layer compared with the pump laser wavelength under tightly focused excitation fields [16-19]. They also indicated that this theoretical concept should be generally applicable to any nonlinear coherent microscopy including THG microscopy [20]. In a previous theoretical study, we also predicted that the epi-THG signals could be attributed to direct backward THG emissions from optically-thin layers [21]. Since the sizes of most organelles and microstructures in epithelial tissues are optically thin with a thickness much less than 1 μm [22,23], the contribution of direct backward THG emission could thus be significant. To estimate the contribution of backscattering, we added 6% acetic acid solution on the mucosa of the live hamster. Acetic acid solution has been widely applied for the clinical diagnosis on cervical and skin pre-cancers [24], and it has also been widely used in the reflection confocal microscopy to provide the nuclear contrast of epithelial cells [25-31]. From previous studies, adding 2%-6% acetic acid solution on the epithelial tissues can greatly increase the backscattering of nuclei in epithelial tissues due to induced compaction of chromatin in nuclei and thus changing the refractive indexes of nuclei [25-37]. In a previous

#70983 - $15.00 USD Received 15 May 2006; revised 6 June 2006; accepted 8 June 2006

work, it was discussed that such compaction of chromatin induced by acetic acid can enhance 100 times of the amount of backscattering from nuclei by using the Mie theory [35]. Therefore, one would expect to see the enhancement on the collected epi-THG signals for layers shallower than the enhanced backscatters (the cell nuclei of the mucosa layers) after adding 6% acetic acid solution on the mucosa of the live hamster. Figures 6(a) and 6(b) show the vertical optical sections of the live hamster oral cavity taken by the epi-THG microscopy before and after adding 6% acetic acid solution on the oral mucosa of the hamster. Upper and lower interfaces of the stratum corneum (SC) can both be clearly observed in Fig. 6, which is a layer shallower than the backscattering cell nuclei. By comparing both images, enhancement on the epi-THG intensity of stratum corneum was not observed after adding 6% acetic acid solution on the mucosa. Our study thus indicates the important contribution of direct backward THG emissions. It is also interesting to notice that the epi-THG signals from the nuclei are greatly enhanced by the addition of the acetic acid solution. An independent study has recently confirmed that acetic acid can serve as a cell nucleus contrast agent in functional THG microscopy [38]. The observed THG signal enhancement in the mucosa layer of Fig. 6(b) could thus partly be attributed to the temporary changes in the linear and nonlinear susceptibilities of the nuclei due to compaction of chromatin after adding acetic acid, causing both forward and direct-backward THG enhancements. From horizontal sections of the intra-vital epi-THG microscopy as shown in Fig. 7, nuclei are clearly outlined after adding 6% acetic acid on the mucosa. This intra-vital study thus further supports the recent finding that acetic acid can be used as the contrast agent of epi-THG microscopy and will be helpful in the future identification of diseases associated with nuclear morphology, such as malignant diseases.

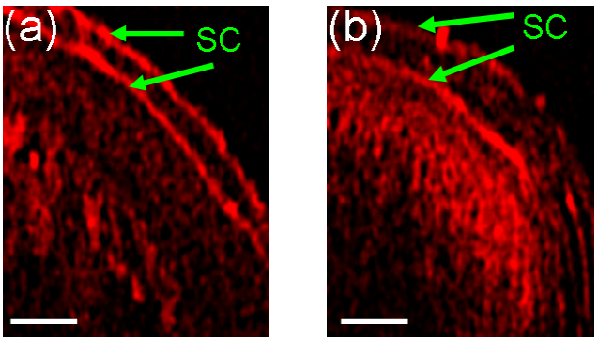


Fig. 6 Vertical sections taken in the live hamster oral cavity by epi-THG microscopy (a) before and (b) after adding 6% acetic acid solution on mucosa. After adding 6% acetic acid solution, the enhanced epi-THG intensity of epithelial cells, except stratum corneum (SC), can be observed. Scale bar: 30μm

#70983 - $15.00 USD
Received 15 May 2006; revised 6 June 2006; accepted 8 June 2006

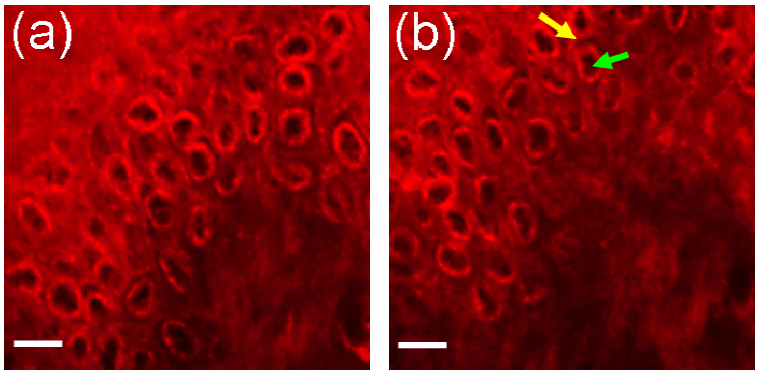


Fig. 7 *In vivo* horizontal sections taken in the mucosa layer of the live hamster oral cavity at different depths by epi-THG microscopy are presented after adding 6% acetic acid solution. The nuclear morphology of squamous cells can be clearly observed by epi-THG microscopy (indicated by green arrow). The yellow arrow indicates the cell membrane. Scale bar: 10μm

## 4. Conclusion

The first *in vivo* virtual biopsy based on epi-THG microscopy is demonstrated using Syrian hamster oral mucosa as a model system. This optical virtual biopsy technique does not require invasive fluorescence staining and the harmonic generation processes leave no energy deposition to the examined tissues. Without complex physical biopsy procedures, it can provide high spatial resolution images of oral mucosa and sub-mucosa in all three dimensions. The demonstrated intra-vital epi-THG microscopy provide high resolution observation of blood flow in the capillary and should be a promising tool to image angiogenesis, which is an important feature of many human diseases including malignancies. The system setup of epi-THG microscopy can be easily integrated with other nonlinear optical microscopy such as SHG and multi-photon fluorescence microscopy by using the same laser system to provide better integrated molecular and structural information for future clinical diagnosis. By applying 6% acetic acid solution on the oral mucosa, enhanced epi-THG contrast on the borders of nuclei can be observed due to the alterations of their linear and nonlinear THG susceptibilities. Our study also supports the fact that direct-backward THG is one of the dominant signals we collected. With a virtual-transition-based technology without using fluorescence, the optical epi-THG biopsy we demonstrated shows a promising future for noninvasive *in vivo* diseases examinations. Combined with the acetic acid that serves as the THG contrast agent for the nuclei, our developed functional epi-THG is especially ideal for the differential diagnosis of diseases associated with nuclear morphology.

## Acknowledgment

The authors gratefully acknowledge financial support from the National Health Research Institute (NHRI-EX95-9201EI) of Taiwan, National Science Council of Taiwan (NSC 94-2314-B-006-067, NSC 94-2120-M-006-004) and the National Taiwan University Center for Genomic Medicine.

#70983 - $15.00 USD
Received 15 May 2006; revised 6 June 2006; accepted 8 June 2006